2019

Understanding the role of Atg7 and Atg14 in autophagy

Ronith Chakraborty

Understanding the role of Atg7 and Atg14 in autophagy

Abstract
Autophagy is the process by which cytosolic components are trafficked to and degraded by the vacuole or lysosome. It plays a critical role in cellular health, aging, cancer, and neurodegenerative diseases. Atg7 and Atgl4 are enzymes required for the autophagic process in Saccharomyces cerevisiae. In this study, we hypothesized that Atg7 controls the size while Atg 14 controls the number of autophagosomes. Using western blotting, Pho8D.60 assay and transmission electron microscopy analysis, we found that Atg7 affects both the size and number of autophagosomes. In addition, we have created cells expressing various levels of Atgl4 using non-native promoters. In addition, we applied the significance of these results to better understand the therapeutic application of mammalian autophagy.

Degree Type
Open Access Senior Honors Thesis

Department
Chemistry

First Advisor
Dr. Steven K. Backues

Second Advisor
Dr. Hedeel Evans

Third Advisor
Dr. Deborah Heyl-Clegg

Keywords
Autophagy, autophagosome, electron mirosocpy, autophagic body, Atg7, Atg 14

Subject Categories
Chemistry

UNDERSTANDING THE ROLE OF ATG7 AND ATG14 IN AUTOPHAGY

By

Ronith Chakraborty

A Senior Thesis Submitted to the

Eastern Michigan University

Honors College

in Partial Fulfillment of the Requirements for Graduation

With Honors in Chemistry

Approved at Ypsilanti, Michigan, on this date May 13, 2019

Supervising Instructor: Dr. Steven K. Backues

Honors Advisor: Dr. Hedeel Evans

Department Head: Dr. Deborah Heyl-Clegg

Associate Director, The Honors College: Dr. Ramona Caponegro

Table of Contents

0.0 Abstract

Autophagy is the process by which cytosolic components are trafficked to and degraded by the vacuole or lysosome. It plays a critical role in cellular health, aging, cancer, and neurodegenerative diseases. Atg7 and Atg14 are enzymes required for the autophagic process in *Saccharomyces cerevisiae*. In this study, we hypothesized that Atg7 controls the size while Atg14 controls the number of autophagosomes. Using western blotting, Pho8Δ60 assay and transmission electron microscopy analysis, we found that Atg7 affects both the size and number of autophagosomes. In addition, we have created cells expressing various levels of Atg14 using non-native promoters. In addition, we applied the significance of these results to better understand the therapeutic application of mammalian autophagy.

1.0 Introduction

Autophagy, which translates to 'self eating,' is a crucial cellular process in which intracellular components are degraded in order to relieve the cell from various stress conditions [1]. Macroautophagy (hereafter referred to as autophagy) is a eukaryotic process where unwanted cellular components are sequestered into a double membrane vesicle referred to as an autophagosome. The autophagosome then fuses to the vacuole (in yeast) or the lysosome (in mammals), where the components are degraded by lysosomal acid proteases. The broken down materials (such as amino acids and other small molecules) that are generated by this degradation are delivered back to the cytoplasm for recycling or as energy resources[2] (Figure 1).

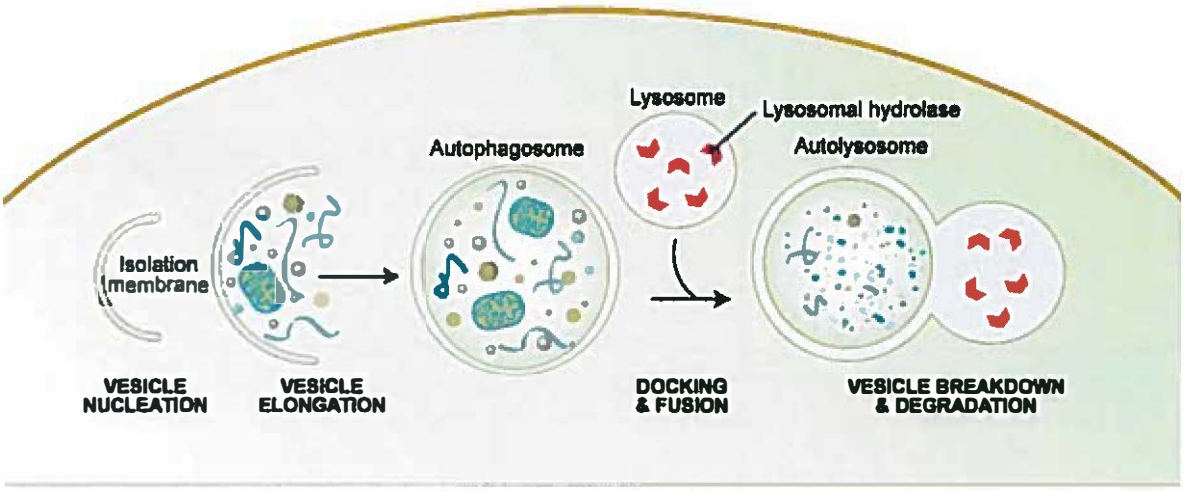

Figure 1: Schematic diagram of autophagy. The process begins the formation of an isolation membrane around the cargo. The membrane expands into an autophagosome and fuses with the vacuole/lysosome for degradation. Figure from Reference 15.

There are two main types of autophagy: selective and non-selective. In selective autophagy, particular components are targeted into the autophagosome for degradation by selective autophagy receptors. These components include damaged organelles (such as mitochondria, endoplasmic reticulum, and peroxisomes), protein aggregates, and intracellular pathogens. However, upon nutrient starvation, cytosolic components are non-selectively sequestered into autophagosomes for degradation, which is known as non-selective autophagy.[3]

Both types of autophagy play an equally important role in maintaining cellular homeostasis and function. Non-selective autophagy allows for the cell to survive during starvation conditions, whereas selective autophagy allows the cell to remove specific unwanted constituents and prolong cellular senescence. These functions give autophagy a key role in preventing diseases such as cancer, neurodegeneration, diabetes, cardiomyopathy, autoimmune diseases, and infections.[4] For example, autophagy is considered to be a tumor-suppressing mechanism during tumor initiation and malignant transformation. The degradation of damaged organelles limits the proliferation of cancerous cells and genomic instability.[5] Also, neurodegenerative diseases, such as Alzheimer's and Parkinson's disease, are due to the aggregation of protein leading to neuronal plaques. This accumulation of aggregated protein can be cleared through autophagic degradation.[6] These studies show the effects on various diseases due to a change in a specific mammalian autophagy gene. However, these studies do not outline the intermediate steps that explain how these genetic changes affect autophagy and thus lead to the disease. Instead,autophagy is more easily studied in model organisms (such as yeast) to be able to determine the molecular steps. This suggests that research on the molecular role of

autophagy proteins in yeast will allow us to better understand the results of mammalian autophagy in disease.

Autophagy requires a variety of autophagy-related (Atg) proteins to occur. Genetic models have been developed in baker's yeast (*Saccharomyces cerevisiae*), which makes it easy to study the molecular role of these proteins. There are approximately 30 Atg proteins that have been identified in yeast, many of which have homologs in humans.[7] There are 18 Atg proteins which are essential for autophagy,[8] and some of them are upregulated during periods of starvation.[9] This suggests that the amount of that protein dictates the amount of autophagy occurring by affecting autophagosome size and/or number. Increasing the size of the autophagosome would increase the volume uptake and would increase autophagic flux since there is more to be degraded. Increasing the number of autophagosomes would also allow for more uptake of cytosolic components and likewise lead to an increase in autophagic flux.

The Klionsky lab tested this idea by looking at the function of an autophagic protein called Atg8. They chose Atg8 since it is one of the core machinery proteins that is upregulated during autophagy and plays a big role in autophagosome formation (Figure 2). First, they created mutant yeast strains with various nonnative promoters in front of the ATG8 gene to control protein levels. Then, they performed a western blot to verify expression levels, a Pho8Δ60 assay to measure the autophagic flux and transmission electron microscopy (TEM) to compare the average size and number of autophagosomes per cell. Using this method, they showed that a decrease in Atg8 protein levels leads to reduced autophagic flux due to a decrease in autophagosome size.[10] In contrast, it was shown by the same method in another study that a decrease in Atg9 levels lead to a decrease in autophagosome number, and not size.[11] This

methodology is very significant as it is currently the only way to determine whether a protein affects autophagosome size vs autophagosome number. The protein's effect on autophagosome size and number can give insight the step of autophagy that the protein is involved in. Therefore, our lab wanted to utilize this novel methodology to help define the roles of other proteins involved in autophagy.

One of the proteins that our lab focused on was Atg7. Atg7 is one of the essential autophagic proteins which is strongly regulated upon nutrient starvation. It is an E1-like activating enzyme required for autophagosome formation and is involved in the Atgl2-5 conjugation and Atg8-PE conjugation system. Atg8 requires an E1 activating enzyme(Atg7), an E2 enzyme (Atg3) and an E3 complex (Atg12-5) to conjugate to phosphoethanolamine (PE). Atg12 also requires an E1 activating enzyme (Atg7) and an E2 enzyme (Atgl0) to conjugate Atg5 (Figure 2). Our group also investigated Atg14, which is a protein involved in the phosphatidylinositol 3-kinase (PI3K) complex. The PI3K complex phosphorylates PI into PI3P, which is a necessary step in autophagosome formation. It also interacts with itself to promote the fusion of autophagosomes with the vacuole/lysosome.[12]

Both Atg7 and Atg14's role in affecting autophagosome size and/or number has not been identified. Our lab used the methodology described above to determine this role. We proposed that Atg7 would affect the size of autophagosomes since Atg7 is upstream of Atg8 and Atg8 controls the size of autophagosomes.[13] Since Atgl4 is responsible for the formation of the autophagosome and is involved upstream in the membrane fusion process.[14] Understanding the molecular roles of these proteins will allow us to better understand the autophagic process,

overall. Understanding this process on a molecular level is a critical step towards the creation of medication which can regulate levels of autophagy, with many potential health benefits.

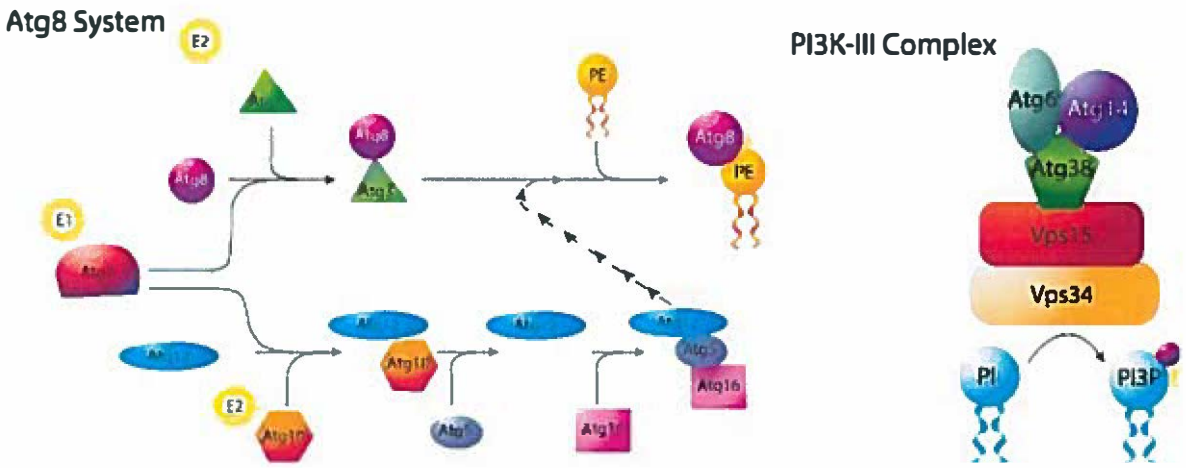

Figure 2: The core autophagic machinery. Atg7 is a part of the Atg8-PE and Atg12-5 conjugation system. The conjugation of Atg8 to PE involves an E1 activating enzyme (Atg7), an E2 enzyme (Atg3) and an E3 complex (Atg12-5). Atg14 is part of the PI3K-III complex and phosphorylates PI to PI3P, which is a necessary step for autophagosome formation. Figure created by Ronith Chakraborty in Adobe Illustrator CC 2017.

2.0 Methodology

2.1 Plasmid Construction

The plasmids used in this study are listed in Table 1, and the primers used are listed in Table 2. Atg7-expressing pRS416 plasmids with distinct promoters[13] were provided as a gift by Dr. Dan Klionsky and were purified using the Quick Plasmid Miniprep kit (Invitrogen). To construct Atg7-expressing pRS406 plasmids, the entire pRS416 plasmid except for the *CEN6* sequence was amplified by PCR using phosphorylated primers (306 and 307) annealing on either side of the *CEN6* sequence. PCR was performed using Phusion Polymerase (NEB) and cleaned up using the NucleoSpin DNA and PCR Clean-up Kit (Macherey-Nagel). The plasmids were ligated by T4 DNA ligase (NEB) and then they were checked for the absence of *CEN6* sequence by PCR using flanking primers (315 and 316).

Atg14-expressing plasmids were created by PA-tagging Atg14 using Longtine-Pringle primers 384 and 385 and a pFA6-PA vector as the template.[16] This tag was then transformed into WLY176 strain and the expression of *ATG14-PA* was verified via western blot with PAP antibodies and the resulting autophagic activity was verified by Pho8Δ60. Atg14-PA including 1000 bp of 5' genomic sequence was amplified out of WLY176 genomic DNA by PCR using primers 309 and 404. To construct pRS406-*ATG14-PA* plasmids, *ATG14-PA* was inserted into pRS406 (linearized by EcoRI and HindIII) using Infusion cloning (In-Fusion® HD EcoDry™ Cloning Kit - Takara Bio). The *ATG14* promoter was then removed from the resulting plasmid, pRS406-*ATG14p-ATG14-PA*, using primers 313 and 418. Then, potential promoters were selected (based on published RNA Sequence data[17]) to give a wide range of Atg14 levels. Those promoters were *ATG1p*, *ATG8p*, *GAL3p*, and *ATG23p* and they were amplified from genomic

yeast DNA using primer pairs (308/416, 324/417, 355/415, and 328/414, respectively) and inserted by Infusion cloning to create the resulting plasmids(11-16).

2.2 Strain Construction

The strains used in this study are listed in Table 3. Yeast transformation and genomic DNA purification were performed using published methods.[18,19] *ATG7* was deleted from FRY143 and WLY176 by homologous recombination with a PCR fragment containing a histidine gene flanked by ~500 bp of *ATG7* 5' and 3' genome sequence. This fragment was generated by PCR using primers (292 and 293) that flank *ATG7* and genomic DNA from an *atg7Δ:: HIS5* strain (YAB292) as a template. The resulting strains (SKB421 and SKB447) were verified by PCR to check for the presence of the *HIS* gene using primers 292 and 311 and the absence of the *ATG7* gene using primers 292 and 312. To integrate *ATG7* under various promoters into the *ura3* locus, each pRS406 plasmid was digested with NcoI enzyme, which made a single cut in the *URA3* gene. The digests were heat killed at 85-90°C for 20 minutes and then transformed into log phase SKB421 and SKB447 to create the desired strains.

ATG14 was deleted from WLY176 by homologous recombination with a PCR fragment containing a kanamycin gene flanked by ~40 bp of *ATG14* 5' and 3' genome sequence. This fragment was generated by PCR using Longtine-Pringle primers (385 and 386) that contained sequences homologous to the 5' and 3' ends of *ATG14* and pFA6-PA as a template[2]. The resulting strain (SKB693) was verified by PCR to check for the presence of a larger band, due to the KAN gene, using primers 405 and 406. To integrate ATG14 under various promoters, the appropriate pRS406 plasmids were digested with StuI or NcoI (for GAL3p), which made a single

cut in the URA3 gene. The digests were then transformed into log phase SKB693 to create the desired strains (SKB738 - SKB747).

2.3 Yeast Culture

Yeast (Saccharomyces cerevisiae) were grown in YPD (1% w/v yeast extract, 2% w/v glucose, 2% w/v peptone) for normal growth conditions and SD-N (0.69 g/L YNB (yeast nitrogen base) without amino acids and ammonium sulfate, 2% w/v glucose) for nitrogen starvation conditions. Nitrogen starvation was induced by harvesting log phase cultures in YPD by centrifugation (2000g for 5 minutes), washing once with sterile water and resuspending in SD-N media. Cultures were grown (starved) for 3 hours until the time of harvest. All cultures were grown at 30°C while being shaken at 300 RPM.

2.4 Western Blotting

About 1 OD of log phase yeast cells in YPD or SD-N were collected by centrifugation and precipitated with 10% ice-cold TCA (trichloroacetic acid) for at least 30 minutes. The samples were pelleted by centrifugation and washed with ice-cold acetone. Pellets were air dried and resuspended in SSB (0.05 M Tris-HCl pH-6.8, 0.2% SDS, 5% glycerol, 0.2% β-mercaptoethanol, 2×10^{-5} % bromophenol blue, in water). The Atg7 samples were run on a 10% SDS-PAGE gel and transferred to a PVDF membrane (Millipore). The power supply, cables, glass plates, SDS-PAGE and transfer apparatus were from BioRad. The membrane was cut at 63 kDa and probed with antibodies in 4% w/v nonfat dairy milk in TBST: 1:10,000 primary mouse anti-Pgkl from Abcam (cat. #22C5D8), 1:5,000 secondary

peroxidase-conjugated goat anti-mouse (cat. #115-035-003), and a 1:10,000 rabbit peroxidase-anti-peroxidase (cat. #323-005-024)) from Jackson ImmunoResearch Laboratories Inc. The Atg14 samples were run on a 15% SDS-PAGE gel and transferred to a PVDF membrane. The membrane was cut at 23 kDa and probed with the following antibodies in 4% w/v nonfat dairy milk in TBST: 1:1,000 primary rabbit anti-histone H3 (ab 1791) antibody from Abcam, 1:5,000 secondary peroxidase-conjugated goat anti-rabbit (cat. #115-035-003) antibody from Millipore, and a 1:2,500 rabbit peroxidase-anti-peroxidase (cat. #323-005-024)) antibody from Jackson ImmunoResearch Laboratories, Inc. Luminata Crescendo Western HRP substrate (Millipore) was used for the detection and the blot was imaged on a BioRad Chemidoc XRS+ system. The resulting blots were quantified using ImageJ.

2.5 Pho8Δ60 Assay

The assay was performed as described[20] with the exception that PMSF was omitted from the lysis buffer to avoid interference with the protein quantification reagent. Protein quantification was performed in a 96 well plate using a BCA assay kit (ThermoFisher) and the absorbances were measured on a BioTek Synergy 2 plate reader. The lysis buffer consisted of the following: 0.02 M PIPES KOH pH 6.8, 0.05 M KCl, 0.1 M KOAc, 0.01 M MgSO4, 0.01 mM ZnSO4, 0.5% TX-100, in water. The reaction buffer used consisted of the following: 0.25 M Tris-HCl pH 8.5, 0.01 M MgSO4, 0.01 mM ZnSO4, and 0.4% TX-100 in water with 0.625 mg/mL para-nitrophenyl phosphate (pNPP).

2.6 Transmission Electron Microscopy (TEM)

Approximately 30 OD of log phase yeast cells were starved for 3 hours in SD-N media. The cells were fixed with $KMnO_4$, dehydrated in acetone, embedded in Spurr's resin, sectioned and imaged by TEM. A Leica UC6 ultramicrotome at the University of Michigan Microscope Image and Analysis Laboratory (U of M MIL) was used to take 70 nm sections of the resin block. The sections were placed onto a 300 mesh copper grid and imaged using a JEOL JSM 1400 Transmission Electron Microscope at the U of M MIL. 6,000x images of the grid square were taken to measure vacuole size in a cell. 30,000x images were taken of vacuoles to measure the size of autophagic bodies. The autophagic bodies and vacuoles were traced using a Wacom Intuos Draw Creative Pen Tablet and Adobe Photoshop CC2017 and the traced bodies were measured using ImageJ (v1.51S, FIJI bundle) by Hayley Cawthon.

Table 1: Plasmids Used in this Study

Plasmids	Name	Tag	Source
1	pRS416-*FLO5p-ATG7-PA*	PA	Bernard *et al.*, 2015
2	pRS416-*GAL3p-ATG7-PA*	PA	Bernard *et al.*, 2015
3	pRS416-*ATG7p-ATG7-PA*	PA	Bernard *et al.*, 2015
4	pRS416-*SEF1p-ATG7-PA*	PA	Bernard *et al.*, 2015
5	pRS406-*FLO5p-ATG7-PA*	PA	Cawthon *et al.*, 2018
6	pRS406-*GAL3p-ATG7-PA*	PA	Cawthon *et al.*, 2018

7	pRS406-*ATG7p-ATG7-PA*	PA	Cawthon *et al.*, 2018
8	pRS406-*SEF1p-ATG7-PA*	PA	Cawthon *et al.*, 2018
9	pRS406-*ATG14p-ATG14-PA*	PA	This study
10	pRS406-*ATG1p-ATG14-PA*	PA	This study
11	pRS406-ATG8p-ATG14-PA	PA	This study
12	pRS406-G*AL3p-ATG14-PA*	PA	This study
13	pRS406-*ATG23p-ATG14-PA*	PA	This study

Table 2. Primers Used in this Study.

Number	Name	Primer	Sequence
292	*ATG7* -500	Forward	GAGGATGCTGAATTAAGACAAAG
293	*ATG7* 500 down	Reverse	CAACGCTTTAGATATGAATGCC
306	pRS416 to 406f	Forward	/5Phos/TAAGAAACCATTATTATCATGACATTAACC
307	pRS416 to 406r	Reverse	/5Phos/CAGGTGGCACTTTTCGG
308	*ATG1p*	Forward	acggtatcgataagcttACCTGCCACAAGGTTATTTCTAC
309	ADH1 terminal	Reverse	ccgggctgcaggaattcGGTGTGGTCAATAAGAGCGAC
311	pUG inner	Reverse	GATCTCTAGACCTAATAAC
312	*ATG7* +500	Reverse	CACCTAACCAGTAATAAAACCTGTAC
313	pRS406 linearization	Reverse	AAGCTTATCGATACCGTCGACC
315	pRS *CEN6* up	Forward	CGGAAATGTTGAATACTCATACTCTTCCC
316	pRS *CEN6* down	Reverse	CATCCGCTTACAGACAAGCTG

324	*ATG8p*	Forward	ggtatcgataagcttCCTTAAAAACTCCATTGAAGACTTTG
328	*ATG23p*	Forward	ggtatcgataagcttAACCAGACCTGGCAAAAC
355	*GAL3p*	Forward	tcgacggtatcgataagcttTTGATGTAAGCGGAGGTGTGG
384	*ATG14-PA* tag	Forward	aacagtcacaggacctcatgaccgatggtacgtggtaggcCGGATCCCCG GGTTAATTAA
385	*ATG14-PA* tag	Reverse	atgcaactttatacacacggcaggaaaaaaagtgcgcactGAATTCGAGCT CGTTTAAAC
386	*ATG14* deletion	Forward	aaagggaagtaaaagttaaaaactagaatcctagtatgacCGGATCCCCGG GTTAATTAA
404	*ATG14* promoter	Forward	acggtatcgataagcttGAGGAAAAACCAATTTGCCTATTACA A AAC
405	*ATG14* flanking	Forward	TCGAAGATGAAAAATGACACTAATTTTGCGCTAATT A
406	*ATG14* flanking	Reverse	ATTGAAACCTTGTTCGACGGCTTTCTTATTTATGGCA AAC
414	*ATG23p*	Reverse	aattgggcaatgcatATTTACTTCTTCACTTTATTTTGTTACC TTATAG
415	*GAL3p*	Reverse	aattgggcaatgcatACTATGTGTTGCCCTACCTTTTTACTTT TA
416	*ATG1p*	Reverse	aattgggcaatgcatTTTCTTAATTTCTCGTCTGGTGTTGTAA AAGAG
417	*ATG8p*	Reverse	aattgggcaatgcatGTCTCTAGTAATTATTTTATTATGATTT TCTCAAC
418	*ATG14* +1	Forward	ATGCATTGCCCAATTTGCCACCATAGAGCG

Table 3. Strains Used in this Study.

Name	Genotype	Source
FRY143	SEY6210 *vps4Δ::TRP1 pep4Δ::LEU2*	Cheong *et al.* 2005
SEY6210	*MATα his3Δ200 leu2-3,112 lys2-801 suc2-Δ9 trp1Δ901 ura3-52*	Robinson Klionsky Emr 1988

SKB421	FRY143 *atg7Δ::HIS5*	Cawthon *et al.*, 2018
SKB447	WLY176 *atg7Δ::HIS5*	Cawthon *et al.*, 2018
SKB461	WLY176 *atg7Δ::HIS5 ura3-52::pRS406-ATG7p-ATG7-PA*	Cawthon *et al.*, 2018
SKB462	WLY176 *atg7Δ::HIS5 ura3-52::pRS406-GAL3p-ATG7-PA*	Cawthon *et al.*, 2018
SKB464	WLY176 *atg7Δ::HIS ura3-52::pRS406-FLO5p-ATG7-PA*	Cawthon *et al.*, 2018
SKB467	WLY176 *atg7Δ::HIS ura3-52::pRS406-SEF1p-ATG7-PA*	Cawthon *et al.*, 2018
SKB478	WLY176 *atg7Δ::HIS5 ura3-52::pRS406*	Cawthon *et al.*, 2018
SKB494	FRY143 *atg7Δ::HIS5 ura3-52::pRS406-ATG7p-ATG7-PA*	Cawthon *et al.*, 2018
SKB495	FRY143 *atg7Δ::HIS5 ura3-52::pRS406-GAL3p-ATG7-PA*	Cawthon *et al.*, 2018
SKB496	FRY143 *atg7Δ::HIS5 ura3-52::pRS406-FLO5p-ATG7-PA*	Cawthon *et al.*, 2018
SKB497	FRY143 *atg7Δ::HIS5 ura3-52::pRS406*	Cawthon *et al.*, 2018
SKB693	WLY176 *atg14Δ::KAN*	This study
SKB738	WLY176 *atg14Δ::HIS5 ura3-52:: pRS406-ATG1p-ATG14-PA* #3	This study
SKB739	WLY176 *atg14Δ::HIS5 ura3-52:: pRS406-ATG8p-ATG14-PA* #1	This study
SKB740	WLY176 *atg14Δ::HIS5 ura3-52:: pRS406-ATG8p-ATG14-PA* #2	This study
SKB741	WLY176 *atg14Δ::HIS5 ura3-52:: pRS406-ATG8p-ATG14-PA* #3	This study
SKB742	WLY176 *atg14Δ::HIS5 ura3-52:: pRS406-ATG8p-ATG14-PA* #4	This study

SKB743	WLY176 *atg14Δ::HIS5 ura3-52:: pRS406-ATG8p-ATG14-PA #6*	This study
SKB744	WLY176 *atg14Δ::HIS5 ura3-52:: pRS406-ATG23p-ATG14-PA #1*	This study
SKB745	WLY176 *atg14Δ::HIS5 ura3-52:: pRS406-ATG23p-ATG14-PA #3*	This study
SKB746	WLY176 *atg14Δ::HIS5 ura3-52:: pRS406-ATG23p-ATG14-PA #4*	This study
SKB747	WLY176 *atg14Δ::HIS5 ura3-52:: pRS406-Galp-ATG14-PA #2*	This study
WLY176	SEY6210 *pho13Δ pho8Δ60*	Kanki *et al.*, 2009
YAB292	YTS158 *atg7Δ::HIS5*	Bernard *et al.*, 2015

3.0 Results

3.1.1 *ATG7* Deletion

To test whether Atg7 levels controlled the size and/or number of autophagosomes, we first had to create mutant yeast which would yield a variety of Atg7 levels. *ATG7* plasmids with various promoters were provided by Dr. Klionsky. However, we first needed to create yeast strains without the native copy of *ATG7*. Homologous recombination was used to delete *ATG7* by using a PCR fragment of a histidine gene with homology to the ends of *ATG7*.

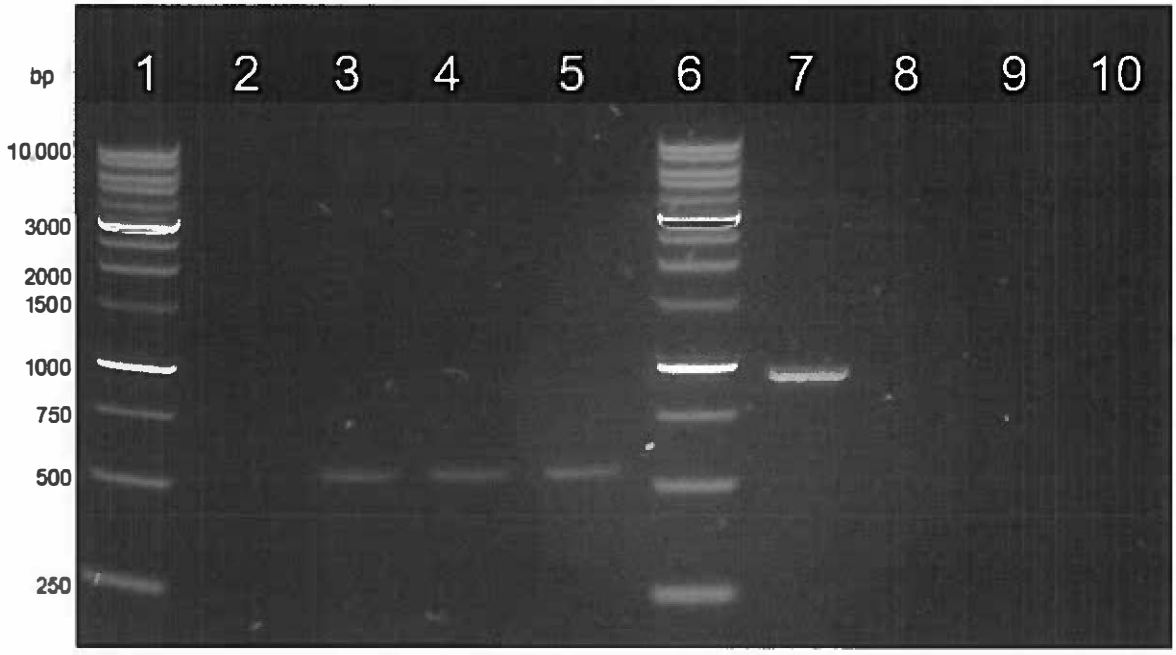

Figure 3. ATG7 deletion in FRY143 strain. PCR and agarose gel electrophoresis was used to verify the deletion of ATG7 from FRY143. Lane 1: Marker. Lane 2: FRY143 wild type. Lane 3: FRY143 *atg7Δ::HIS5* clone 2. Lane 4: FRY143 *atg7Δ::HIS5* clone 2. Lane 5: *atg7Δ::HIS5*. Lane 6: Marker. Lane 7: FRY143 wildtype. Lane 8: FRY143 *atg7Δ::HIS5* clone 2. Lane 9: FRY143 *atg7Δ::HIS5* clone 5. Lane 10: *atg7Δ::HIS5*. Primers 292/311 (detects *HIS5*) were used for lanes 2-5 and primers 292/312 (detects *ATG7*) were used for lanes 7-10.

This deletion of *ATG7* from the FRY143 strain was verified by PCR and gel electrophoresis as shown in Figure 3. Genomic yeast DNA from putative clones was used in a PCR with the following sets of primers: 292/311 and 292/312. The first set of primers (292/311) detected the presence of the histidine gene whereas the second set of primers(292/312) were used to verify the removal of *ATG7*. The presence of the bands on the left (Lanes 3-5) shows the presence of the histidine gene. The absence of bands on the right (Lanes 8-10) shows that *ATG7* was knocked out. The same methodology was used to verify *ATG7* deletion in WLY176 (data not shown).

3.1.2 Conversion of pRS416 to pRS406

The plasmid pRS416 contains a *CEN6* sequence, which is the origin of replication in yeast and allows multiple copies of plasmids to be present in the final strains. Multiple copies would lead to inconsistent levels of *ATG7* expression. Therefore, the *CEN6* sequence was removed from pRS416 plasmids containing *ATG7* to create the corresponding pRS406 plasmids. This was done by amplifying the plasmid, with the exception of the *CEN6* sequence, by PCR. The resulting linearized plasmids were then re-circularized by ligation and checked by PCR with primers that flank the *CEN6* sequence, as shown in Figure 4. The negative control (pRS416-CUp-PA) is the linearized plasmid with the *CEN6* sequence and is represented by the band in Lane 2 at ~750 bp. Lane 3-12 contained circular plasmids without the *CEN6* sequence, which yielded bands at ~250 bp. The smaller band size verifies that the *CEN6* was removed.

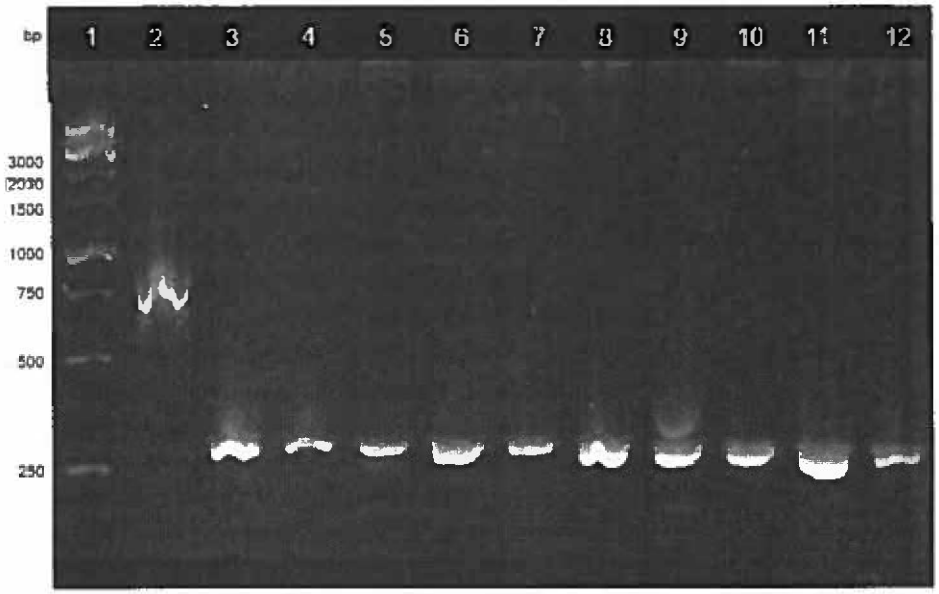

Figure 4. Conversion of pRS416 to pRS406. PCR products used to verify that the CEN6 sequence was removed from the pRS416 plasmid were separated on an agarose gel. Lane 1: 1 kb Ladder. Lane 2: pRS416-CUp-PA (negative control). Lane 3: *ATG7p* clone 1. Lane 4: *ATG7p* clone 2. Lane 5: *GAL3p* clone 1. Lane 6: *GAL3p* clone 2. Lane 7: *FLO5p* clone 1. Lane 8: *FLO5p* clone 2. Lane 9: *SEF1p* clone 1. Lane 10: *SEF1p* clone 2.

3.1.3 Expression of Atg7 Using Mutant Strains

The pRS406 plasmids containing *ATG7* under different promoters were integrated into FRY143 *atg7Δ::HIS5* yeast to create strains expressing different levels of *ATG7*. Cultures of each strain were analyzed by western blot to verify the level of *ATG7* expression (Figure 5).

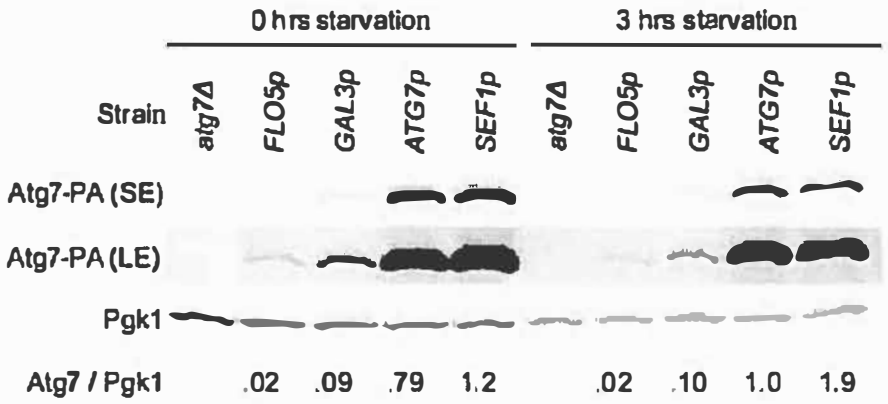

Figure 5. Western blot of WLY176 mutant strains expressing various levels of Atg7. *ATG7p* is the native promoter, while *atg7Δ* is the negative control. Samples were processed at 0-hour starvation and 3 hours starvation in SD-N. Pgk1 was used as a loading control.

Each lane contains a mutant strain with *ATG7-PA* expressed under a different promoter. The PA is the Protein A tag and it allows for the visualization of Atg7 on a western blot. The size and intensity of the bands indicate the amount of Atg7 protein expression. The quantification shows that the Atg7 expression levels are approximately the same when comparing 0 hours and 3 hour starvation periods. It is also shown that there is an increase in Atg7 levels as the strength of the promoter is increased.

3.1.4 Atg7 Levels Affect Autophagic Flux

Having demonstrated that different promoters caused a change in Atg7 levels, we then performed a Pho8Δ60 assay to show the effect of different Atg7 levels on autophagic activity.

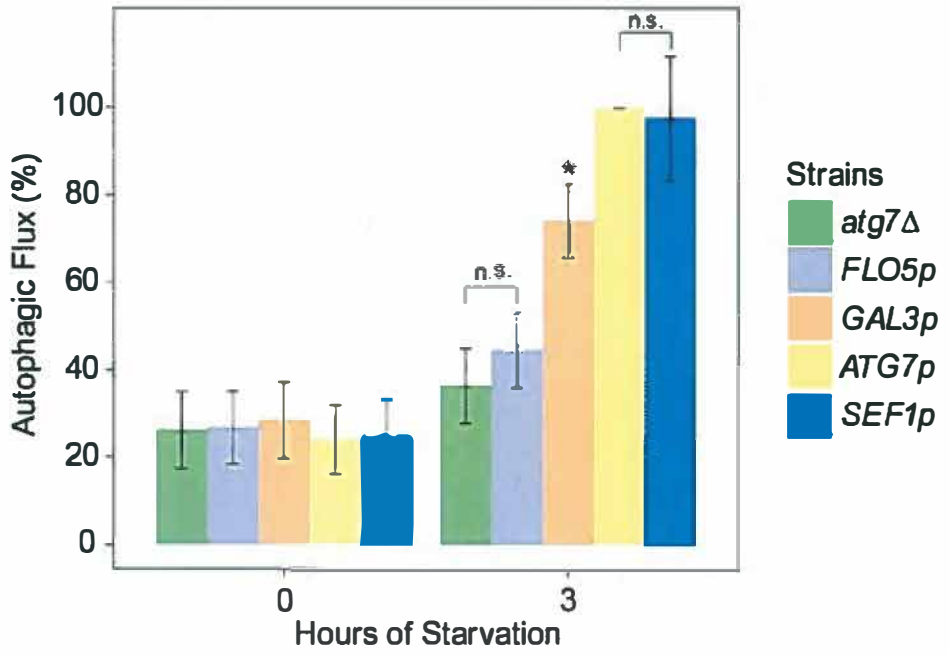

Figure 6. The autophagic activity of mutant *ATG7* strains with different promoters. The mutant strains were analyzed by Pho8Δ60 assay to measure total autophagic flux. The protein concentration was also measured in order to determine the amount of autophagic flux per unit of protein. These were normalized to the *ATG7p* (native promoter) at 3-hour starvation to give a percentage of autophagic activity compared to wild type Atg7.

The mutant strains show approximately the same amount of autophagic activity under nutrient-rich conditions (0-hour starvation). However, after 3 hours of nitrogen starvation, the autophagic activity increased as the strength of the promoters increased. This shows that the increasing Atg7 leads to an increase in autophagic flux and that autophagy is upregulated under starvation conditions. Lastly, the effect of the *ATG7p* and *SEF1p* on Atg7 expression levels seemed to be very similar and there was no significant difference in autophagic activity. Therefore, *SEF1p* was omitted for the rest of the experiments.

3.1.5 Atg7 Affect Size and Number of Autophagosomes

After determining that increasing Atg7 levels increases autophagic flux, we tested whether this occurred due to a change in the size and/or the number of autophagosomes. Samples were imaged using transmission electron microscopy as shown in Figure 7.

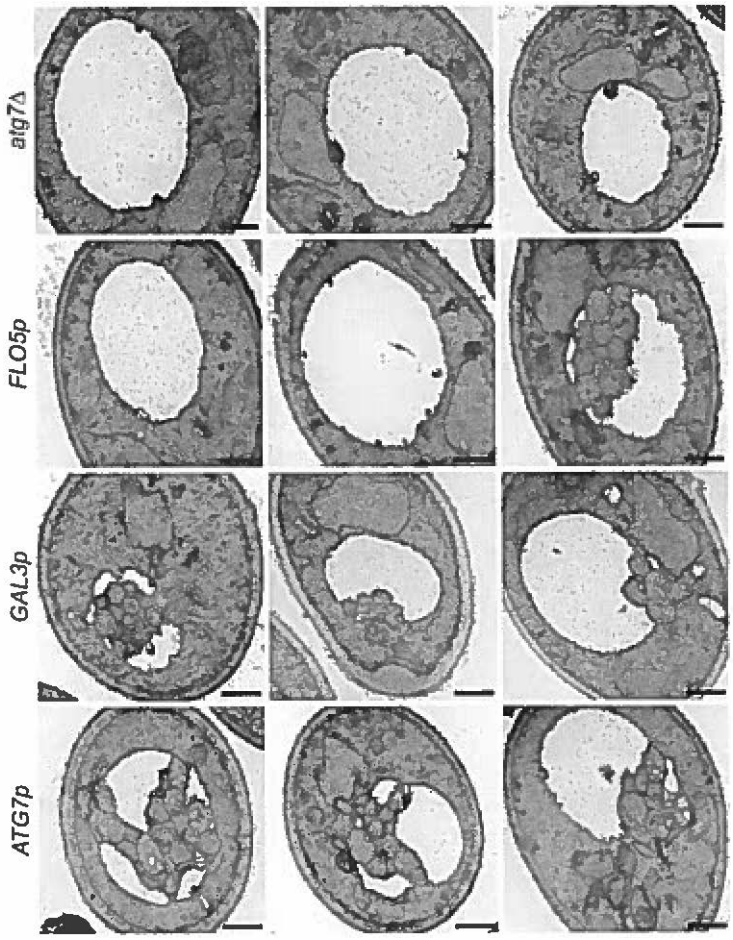

Figure 7. TEM images of Atg7 mutant strains. Images were taken after cells were starved for 3 hours in SD-N. Each image is taken at 30,000x magnification. Scale bar~600 nm. Figure from *Cawthon et al.*, ref 21.

Cells with no Atg7 (*atg7Δ*) showed the least amount of autophagic bodies. As we increased the strength of the promoters (Atg7 protein levels), we saw an increase in the numbers of autophagosomes in the vacuoles. The images were analyzed to measure the average autophagic body volume and the average number of autophagic bodies per cell from each strain as described in the methodology. After analysis, it was found that Atg7 levels affected both the size and number of autophagosomes as shown in Figures 8 and 9.

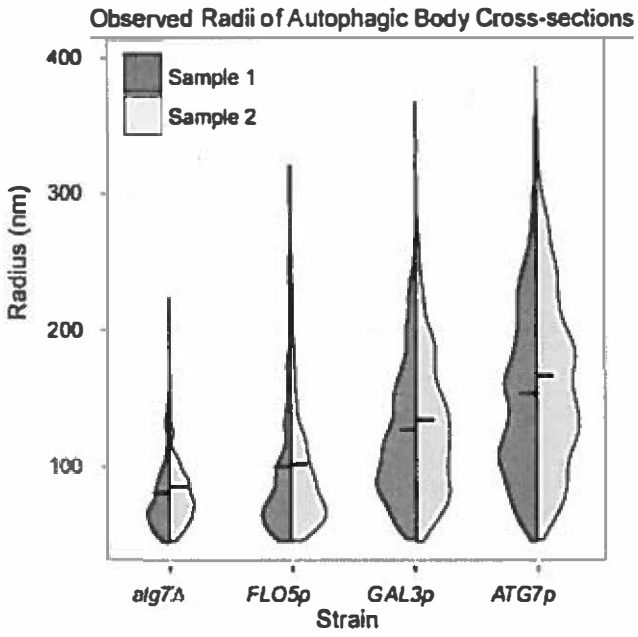

Figure 8. Observed radii of autophagic bodies in Atg7 mutant strains. Split violin plot shows the cross section radii of autophagic bodies from TEM analysis. The horizontal bars represent the mean radius. Sample 1 and Sample 2 were imaged independently and their data were compared. Figure from *Cawthon et al.*, ref 21.

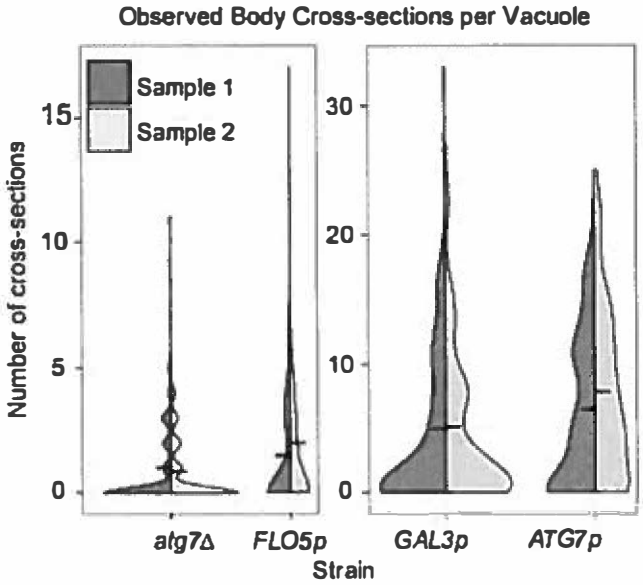

Figure 9. Observed number of cross-sections of autophagic bodies per vacuole. Split violin plot shows the number of body cross-section in a cell determined from TEM analysis. The horizontal bars represent the mean number of body cross-sections per cell. Sample 1 and Sample 2 were imaged independently and their data were compared. Figure from *Cawthon et al.*, ref 21.

The data from the microscopy was also fitted to a mathematical model that estimated the average size and number of autophagic bodies per mutant Atg7 strain, as shown in Figure 10.

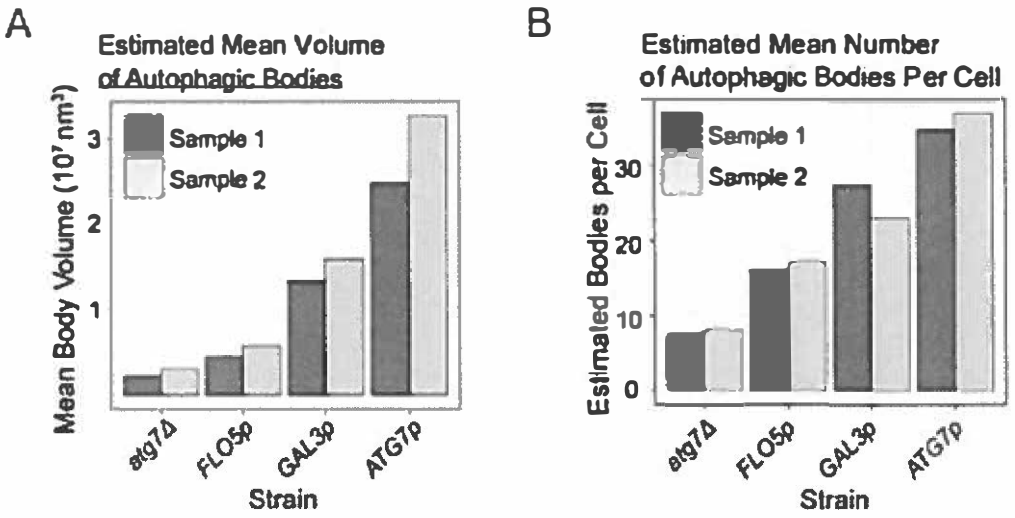

Figure 10. The estimated mean volume of autophagic bodies. All mutant strains were grown and starved in SD-N for 3 hours. They were then prepped and imaged by TEM. (A)The images were analyzed and the data were fitted to a mathematical model, which estimated the mean autophagic body volume. (B) The image analysis data was also fitted to a mathematical model to estimate the mean number of autophagic bodies per cell. Sample 1 and Sample 2 were imaged independently and their data were compared. Figure from *Cavthon et al.*, ref 21.

Both sets of samples showed similar results for each mutant strain. These mathematical model also showed that both the volume and number of autophagic bodies increased as the amount of Atg7 increased. This trend was consistent with the trend seen in the raw data. This concludes that Atg7 affects the size and number of autophagosomes during nonselective autophagy. The same methodology was then used to study Atg14, a protein that is involved in autophagosome formation.

3.2.1 *ATG14* Deletion

The first step to creating strains containing various levels of *ATG14* was to delete the native copy *ATG14* from the WLY176 strain). Homologous recombination was used to delete *ATG14* by using a PCR fragment of a kanamycin gene with homology to both ends of *ATG14*. This deletion was verified by PCR and gel electrophoresis as shown in Figure 9.

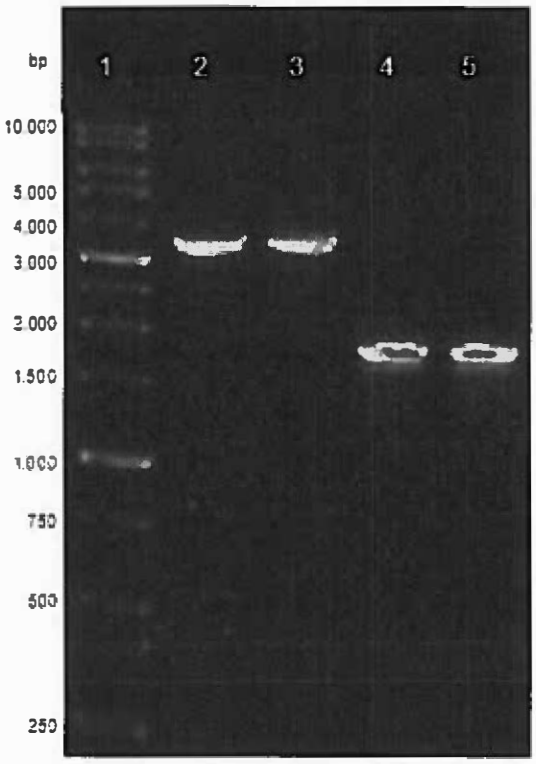

Figure 12. Deletion of ATG14 in WLY176 strain. PCR using primers (404 and 406), which anneal on either side of the *ATG14* gene, was used to verify that *ATG14* was knocked out of WLY176. Lane 1: Ladder. Lane 2 and 3: WLY176 wild type. Lanes 4 and 5: putative WLY176 *atg14Δ:: KAN* clones.

The presence of the bands around ~4,000 bp signifies wild type WLY176 which contains ATG14. The bands at ~1,500 bp represent WLY176 *atg14Δ::kan*. The smaller size of the WLY176 *atg14Δ::KAN* verifies that *ATG14* was removed and replaced with a kanamycin gene.

3.2.2 PA tagging ATG14

In a separate WLY176 strain, *ATG14* was also tagged with Protein A (PA) tag using primers 384 and 385. The tagging allows Atg14 to be recognized on a western blot. To make sure the tagging did not affect the activity of Atg14 in non-selective autophagy, we performed a Pho8Δ60 assay as shown in Figure 13.

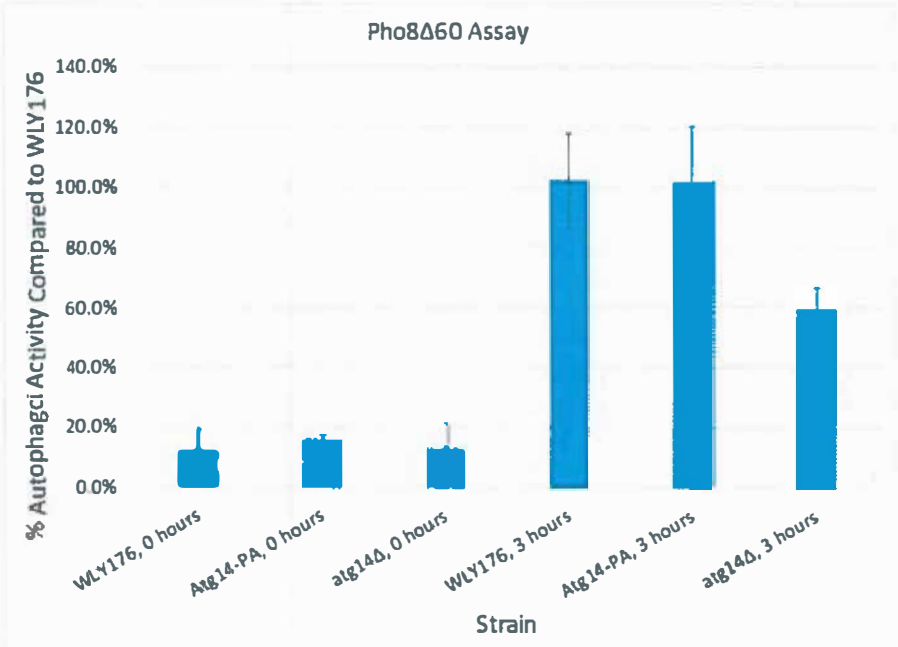

Figure 13. Pho8Δ60 assay to verify autophagic flux in the *ATG14-PA strain*. The autophagic activity of wild type WLY176 was compared against the Atg14-PA and *atg14Δ* strains under normal and 3-hour nitrogen starvation conditions. N = 4. Error bars represent 95% confidence interval.

The Pho8Δ60 assay compared the autophagic activity of wild type WLY176, *ATG14-PA*, and *atg14Δ* strains under normal (0-hour) and 3-hour nitrogen starvation conditions. Under normal conditions, all three of the strains show approximately identical low levels of autophagic activity. However, upon the 3-hour nitrogen starvation, only the wild type WLY176 and the *ATG14-PA* strain had similar levels. This shows that the PA tag does not affect Atg14's ability in selective autophagy. The *atg14Δ* strain exhibited significantly lower levels of autophagic activity than the other two strains, verifying the importance of Atg14 in autophagy.

3.2.3 Expression of Atg14 Under Different Promoters

After the PA-tagging of *ATG14*, promoters were picked based on published RNA sequence data to create a variety of Atg14 protein levels. The chosen promoters (*ATG1p*, *ATG8p*, *ATG23p*, and *GAL3p*) were amplified from genomic yeast DNA and inserted into plasmids containing *ATG14-PA* which were used to create mutant Atg14 strains. Next, we performed a western blot to test whether these promoters gave a variety of Atg14 expression, as shown in Figure 14.

Figure 14. Western blot to verify Atg14 levels. Western blot was performed to verify that strains with various promoters gave distinct expression of *ATG14*. Lane 1: *ATG14p* (positive control). Lane 2: *ATG1p*. Lane 3: *ATG8p* clone 1. Lane 4: *ATG8p* clone 2. Lane 5: *ATG23p* clone 1. Lane 6: *ATG23p* clone 2. Lane 7: *GAL3p*. Lane 8: *atg14Δ* (negative control).

According to the western blot, each promoter shows distinct levels of Atg14 expression. This level of Atg14 expression was determined by the size and intensity of the band. The clones showed that the non-native promoter was consistent in Atg14 expression. *ATG1p* showed the greatest expression followed by *ATG8p*, *ATG23p*, *ATG14p*, and *GAL3p*.

Now that strains have been found that express different levels of Atg14, more Pho8Δ60 assays will be performed to test Atg14's effect on autophagic activity. Afterward, TEM image analysis will be performed to see whether any change in activity is due to the change in autophagosome size and/or number.

4.0 Discussion

4.1 Atg7 Results

In this paper, we examined whether Atg7 affects nonselective autophagic activity in yeast and whether this is due to regulating the size and/or number of autophagosomes. Atg7 was chosen because it is essential for autophagy to occur and is involved in the Atg12 and Atg8 conjugation pathways. Determining Atg7's function can help us understand the function of the Atg8 system. We hypothesized that Atg7 regulates nonselective autophagy by controlling the size of autophagosomes.

To test this hypothesis, different levels of Atg7 needed to be expressed. Atg7 plasmids gifted from Dr. Dan Klionsky contained different promoters, which would vary *ATG7* expression. The Atg7 plasmids were successfully converted from pRS416 to pRS406 plasmids to minimize cell-to cell variation and integrated into the WLY176 and FRY143 strains. The expression levels of Atg7 were verified by western blot and gave a gradient of expression levels. FLO5p showed the least Atg7 expression and required multiple blots with stronger antibody dilutions to verify its presence. *GAL3p* showed a higher expression that *FLO5p* and *ATG7p* (native promoter) showed an even higher level of expression. *SEF1p* showed slightly higher expression levels than *ATG7p*.

Afterward, multiple Pho8Δ60 assays were performed to measure the autophagic flux of the mutant Atg7 strains at basal conditions and at 3 hours starvation. It was determined that as Atg7 protein levels increased, this lead to an increase in autophagic flux. FLO5p had the least protein and thus the least activity, GAL3p had more protein and more activity, etc. Since *ATG7p* and SEF1p were shown to have very similar Atg7 expression and autophagic activity, SEF1p

was omitted from further analysis. The question remained of whether Atg7 caused this increase in flux by contributing to an increase in the size or number of autophagosomes. This was determined by TEM image analysis.

The TEM images of the Atg7 mutant strains verified that the increase in Atg7 leads to an increase in autophagic activity, due to an increase in both the size and number of autophagosomes. The change in autophagosome size was expected since Atg8, which is downstream of Atg7, has been shown to affect the size of autophagosomes. It was also previously known that decreasing Atg7 leads to a decrease in Atg8 conjugation to PE.[13] However, it was surprising to see that Atg7 affected the number of autophagosomes. This could possibly mean that the conjugation of Atg12 to Atg5 affects the number of autophagosomes formed. To determine if this were true, Atgl2 and Atg5 could be investigated using the same methodology we used for Atg7.

4.2 Atg7 Medical Relevance

A paper by Komatsu *et al.* described that mammalian Atg7 was shown to be a homolog of the yeast Atg7[23]. This suggests that the results regarding Atg7 in yeast could directly translate to autophagy in mammals. This is significant, as it suggests that Atg7 might regulate mammalian autophagy by controlling the size and number of autophagosomes. Atg7 has been implicated in various pathologies such as neurodegenerative diseases, cancer, infectious disease, and cardiovascular diseases - this research implies that regulating the expression of Atg7 could be a therapy for these diseases.

Neurodegenerative diseases, such as Huntington's and Parkinson's, are incurable conditions that result in progressive deterioration and death of nerve cells. This deterioration is caused by the aggregation of misfolded proteins. Autophagy is one of the major intracellular mechanisms which can degrade misfolded proteins and maintain proteostasis. A paper by Gao *et al*. showed that lack of Atg7, which decreases autophagy, leads to an accumulation of p62. The accumulation of p62 promotes the aggregation of proteins and therefore, leads to neurodegenerative diseases.[24] It has also been shown that the deletion of Atg7 in the brain leads to a reduction of midbrain dopaminergic (mDA) neurons. This is crucial because Parkinson's disease is caused by a gradual loss of mDA neurons during aging.[25] This suggests that an increase in Atg7 can clear up the p62 accumulation and protein aggregates.

Atg7 has also been implicated in cancer development. The two main characteristics of cancer are uncontrollable proliferation and suppression of apoptosis. Atg7 has been shown to have various roles in different cancers. For example, it has been shown that the increase of Atg7 decreases the resistance of human breast cancer cells to photodynamic therapy[26] and promotes actions of tetrandrine, a bisbenzylisoquinoline alkaloid which exhibits potent anti-tumor effects in human hepatocellular carcinoma.[27] This shows how Atg7 can act as a tumor suppressor. However, Atg7 has also been shown to be an oncogene. For example, the overexpression of *ATG7* leads to the inhibition of p27, causing G2-M transition and growth of human bladder cancer cells.[28] It has also been shown that Atg7 deficiency produces an autophagy-deficient phenotype, shown by the accumulation of p62, enlarged ER, and a large cytoplasm. This deficiency leads to inhibition of PTEN (phosphate and tensin homolog)-deficient prostate tumor growth through protein

homeostasis.[29] Overall, this shows how Atg7 can act as an oncogene or a tumor suppressor, based on the type of cancer.

In recent years, the role of autophagy in immunity has become of great interest. *ATG7*, in particular, has been shown to play various roles in different infectious diseases. For example, the knockout of *ATG7* has lead to a quicker spread of *Pseudomonas aeruginosa* infection in mice, which can cause an accumulation of p62, increased inflammatory response, and increased mortality.[30] This suggests that Atg7 is critical for controlling *P. aeruginosa* infection and may be a negative regulator of the inflammatory response. It was also established that Atg7 deficiency prevents the clearance of *Mycobacterium tuberculosis* by human immunity-related GTPase family M protein.[31] This is significant because *M. tuberculosis* is the causative agent of tuberculosis and has shown resistance to current antibiotics. A potential therapeutic could involve increasing Atg7 concentrations to upregulate autophagy and efficiently eliminate *M. tuberculosis*.[32] Atg7 has also been implicated in human papillomavirus (HPV) and hepatitis C virus (HCV) research. The knockdown of *ATG7* has shown to significantly enhance the infectivity of HPV in natural host cells (primary human keratinocytes).[33] However, it was also shown that suppression of Atg7 expression suppresses the replication of HCV RNA[34] and results in apoptosis of HCV-infected human hepatocytes.[35] This suggests that an increase in Atg7 or autophagy plays a positive role in facilitating HCV infection.

Together, this research shows how Atg7 plays different roles in various pathologies. In neurodegenerative diseases, overexpression of Atg7 can be used to clear up p62 accumulation

and protein aggregates through upregulation in autophagy. However, the role of Atg7 varies in cancer and infectious diseases. Atg7 can either act as an oncogene or a tumor suppressor depending on the type of cancer and the stage of progression. In terms of infectious diseases, Atg7 can either suppress infections or promote it, depending on the type of infectious disease. Ultimately, this shows that Atg7-dependent therapeutics can be designed to treat diseases from different pathologies. Our results show that Atg7 controls both autophagosome size and number, unlike Atg8 or Atg9, which either controls autophagosome size or number, respectively. Therefore, causing a deficiency of Atg7 might be useful as a therapeutic for certain cases. Further studies will be required to determine whether Atg7's ability to control both autophagosome size and number makes it an efficient target of therapy in various pathologies.

4.3 Atg14 Results

We also looked at determining the function of Atg14 using the same methodology as Atg7. First, we successfully PA-tagged Atg14 and verified its expression by western blot. However, we ran into an issue with the western blot: the size of the Atg14-PA was too close to that of the loading control Pgk1, and this would prevent accurate quantification of Atg14 levels. The loading control was important since it ensured that any changes we saw in protein levels was due to the expression of the gene and not because of the volumes of sample loaded. To solve this issue, we used a smaller loading control, histone H3.

Next, we had to create the mutant Atg14 strains with various promoters, unlike the Atg7 plasmids, which were given to us as a gift. The following promoters were picked based on RNA expression data: *ATG1p*, *ATG8p*, *ATG23p*, and *GAL3p*. A western blot was performed to verify

the expression levels of Atg14 under different promoters. It initially appeared as if these promoters did not function properly, because some promoters displayed two PA bands (data not shown), rather than the one band expected. After performing plasmid sequence analysis, it was found that these plasmids did not contain a promoter in front of ATG14. The presence of two PA bands was odd since the absence of a promoter would usually lead to minimal expression, but ultimately the same conclusion was made: we needed to try again at creating mutant strains. We picked new plasmid clones, verified that they contained the appropriate promoter, and transformed them into the WLY176 strain. A western blot was then performed on the new Atg14 strains. It was found that *ATG1p* showed the highest Atg14 expression, followed by *ATG8p*, *ATG23p*, and *ATG14p* (native promoter). *GAL3p* did not show any Atg14 expression as indicated by the lack of a band. However, there may be Atg14 present and its presence is difficult to see due to the strong bands nearby. Future analysis will involve performing western blots where *GAL3p-ATG14*-PA samples are treated with stronger antibody concentrations to detect Atg14.

5.0 Conclusions

It was hypothesized that essential autophagy proteins Atg7 and Atg14 play a role in controlling autophagy, where Atg7 controls the size and Atg14 controls the number of autophagosomes. A gradient of Atg7 protein levels was created by using non-native promoters and verified by western blot. The autophagic activity was measured by Pho8Δ60 assay and the autophagosomes size and number were analyzed by transmission electron microscopy (TEM). It was found that a decrease in Atg7 decreased non-selective autophagy and decreased both the size and number of autophagosomes. Atg14 was also subjected to the same methodology. Various levels of Atg14 were successfully expressed using non-native promoters. Next, the mutant Atg14 strains will be tested for autophagic activity to determine the effects of the amount of Atg14 on non-selective autophagy.

6.0 References

1. Suzuki, Hironori, et al. "Structural Biology of the Core Autophagy Machinery." *Current Opinion in Structural Biology*, vol. 43, 2017, pp. 10–17., doi:10.1016/j.sbi.2016.09.010.
2. Feng, Yuchen, et al. "The Machinery of Macroautophagy." *Cell Research*, vol. 24, no. 1, 2013, pp. 24–41., doi:10.1038/cr.2013.168.
3. Mijaljica, Dalibor, et al. "The Intriguing Life of Autophagosomes." *International Journal of Molecular Sciences*, vol. 13, no. 3, 2012, pp. 3618–3635., doi:10.3390/ijms13033618.
4. Cianfanelli, Valentina, and Francesco Cecconi. "Developmental Autophagy." *Autophagy in Health and Disease*, 2013, pp. 103–116., doi:10.1016/b978-0-12-385101-7.00007-3.
5. Bhutia, Sujit K et al. "Autophagy: cancer's friend or foe?." *Advances in cancer research* vol. 118 (2013): 61-95. doi:10.1016/B978-0-12-407173-5.00003-0
6. Guo, Fang et al. "Autophagy in neurodegenerative diseases: pathogenesis and therapy." *Brain pathology (Zurich, Switzerland)* vol. 28,1 (2017): 3-13. doi:10.1111/bpa.12545
7. Nakatogawa, Hitoshi, et al. "Dynamics and Diversity in Autophagy Mechanisms: Lessons from Yeast." *Nature Reviews Molecular Cell Biology*, vol. 10, no. 7, 2009, pp. 458–467., doi:10.1038/nrm2708.
8. Longatti, A, and S A Tooze. "Vesicular Trafficking and Autophagosome Formation." *Nature News*, Nature Publishing Group, 17 Apr. 2009, www.nature.com/articles/cdd200939.
9. Bartholomew, Clinton R et al. "Ume6 transcription factor is part of a signaling cascade that regulates autophagy." *Proceedings of the National Academy of Sciences of the United States of America* vol. 109,28 (2012): 11206-10. doi:10.1073/pnas.1200313109
10. Xie, Zhiping, et al. "Atg8 Controls Phagophore Expansion during Autophagosome Formation." *Molecular Biology of the Cell*, vol. 19, no. 8, 2008, pp. 3290–3298., doi:10.1091/mbc.e07-12-1292.
11. Jin, Meiyan et al. "Transcriptional regulation by Pho23 modulates the frequency of autophagosome formation." *Current biology: CB* vol. 24,12 (2014): 1314-1322. doi:10.1016/j.cub.2014.04.048
12. Geng, Jiefei, and Daniel J. Klionsky. "The Atg8 and Atg12 Ubiquitin-like Conjugation Systems in Macroautophagy. 'Protein Modifications: Beyond the Usual Suspect/s' Review Series." *EMBO Reports*, vol. 9, no. 9, 2008, pp. 859–864., doi:10.1038/embor.2008.163.

13. Bernard, Amélie, and Daniel J Klionsky. "Rph1 Mediates the Nutrient-Limitation Signaling Pathway Leading to Transcriptional Activation of Autophagy." *Autophagy*, vol. 11, no. 4, 2015, pp. 718–719., doi:10.1080/15548627.2015.1018503.
14. Obara, Keisuke, and Yoshinori Ohsumi. "Atg14: A Key Player in Orchestrating Autophagy." *International Journal of Cell Biology*, vol. 2011, 2011, pp. 1–7., doi:10.1155/2011/713435.
15. Meléndez, Alicia. "Figure 1, Schematic Diagram of the Steps of Autophagy. - WormBook - NCBI Bookshelf." WormBook: The Online Review of C. Elegans Biology [Internet]., U.S. National Library of Medicine, 1 Jan. 1970, www.ncbi.nlm.nih.gov/books/NBK116074/figure/autophagy_figure1/.
16. Longtine, Mark S., et al. "Additional Modules for Versatile and Economical PCR-Based Gene Deletion and Modification in Saccharomyces Cerevisiae." *Yeast*, vol. 14, no. 10, 1998, pp. 953–961., doi:10.1002/(sici)1097-0061(199807)14:10<953::aid-yea293>3.3.co;2-l.
17. Backues, Steven K, et al. "Estimating the Size and Number of Autophagic Bodies by Electron Microscopy." *Autophagy*, vol. 10, no. 1, 10 Jan. 2013, pp. 155–164., doi:10.4161/auto.26856.
18. Gietz, R Daniel, and Robert H Schiestl. "Large-Scale High-Efficiency Yeast Transformation Using the LiAc/SS Carrier DNA/PEG Method." Nature Protocols, vol. 2, no. 1, 2007, pp. 38–41., doi:10.1038/nprot.2007.15.
19. Lõoke, Marko et al. "Extraction of genomic DNA from yeasts for PCR-based applications." *BioTechniques* vol. 50,5 (2011): 325-8. doi:10.2144/000113672
20. Noda, Takeshi, and Daniel J. Klionsky. "Chapter 3 The Quantitative Pho8Δ60 Assay of Nonspecific Autophagy." *Methods in Enzymology Autophagy: Lower Eukaryotes and Non-Mammalian Systems, Part A*, 2008, pp. 33–42., doi:10.1016/s0076-6879(08)03203-5.
21. Cawthon, Hayley, et al. "Control of Autophagosome Size and Number by Atg7." *Biochemical and Biophysical Research Communications*, vol. 503, no. 2, 5 Sept. 2018, pp. 651–656., doi:10.1016/j.bbrc.2018.06.056.
22. Kanki, Tomotake, et al. "Atg32 Is a Mitochondrial Protein That Confers Selectivity during Mitophagy." *Developmental Cell*, U.S. National Library of Medicine, July 2009, www.ncbi.nlm.nih.gov/pubmed/19619495.
23. Komatsu, Masaaki, et al. "Impairment of Starvation-Induced and Constitutive Autophagy in Atg7-Deficient Mice." *JCB*, Rockefeller University Press, 9 May 2005, jcb.rupress.org/content/169/3/425.long.
24. Gao, Wentao et al. "E1-like activating enzyme Atg7 is preferentially sequestered into p62 aggregates via its interaction with LC3-I." *PloS one* vol. 8,9 e73229. 4 Sep. 2013, doi:10.1371/journal.pone.0073229.
25. Niu, Xue-Yuan, et al. "Deletion of Autophagy-Related Gene 7 in Dopaminergic Neurons Prevents Their Loss Induced by MPTP." *Neuroscience*, vol. 339, 17 Dec. 2016, pp. 22–31., doi:10.1016/j.neuroscience.2016.09.037.

26. Xue, Liang-Yan et al. "Atg7 deficiency increases the resistance of MCF-7 human breast cancer cells to photodynamic therapy." *Autophagy* vol. 6,2 (2010): 248-55.
27. Gong, Ke et al. "Autophagy-related gene 7 (ATG7) and reactive oxygen species/extracellular signal-regulated kinase regulate tetrandrine-induced autophagy in human hepatocellular carcinoma." *The Journal of biological chemistry* vol. 287,42 (2012): 35576-88. doi:10.1074/jbc.M112.370585
28. Zhu, Junlan, et al. "ATG7 Overexpression Is Crucial for Tumorigenic Growth of Bladder Cancer In Vitro and In Vivo by Targeting the ETS2/miRNA196b/FOXO1/p27 Axis." *Molecular Therapy - Nucleic Acids*, vol. 7, 16 June 2017, pp. 299–313., doi:10.1016/j.omtn.2017.04.012.
29. Santanam, Urmila et al. "Atg7 cooperates with Pten loss to drive prostate cancer tumor growth." *Genes & development* vol. 30,4 (2016): 399-407. doi:10.1101/gad.274134.115
30. Li, Xuefeng, et al. "Atg7 enhances host defense against infection via downregulation of superoxide but upregulation of nitric oxide." *Journal of immunology (Baltimore, Md. : 1950)* vol. 194,3 (2014): 1112-21. doi:10.4049/jimmunol.1401958
31. Singh, Sudha B, et al. "Human IRGM Induces Autophagy to Eliminate Intracellular Mycobacteria." *Science (New York, N.Y.)*, U.S. National Library of Medicine, 8 Sept. 2006, www.ncbi.nlm.nih.gov/pubmed/16888103/.
32. Gutierrez, Maximiliano G. et al. "Autophagy Is a Defense Mechanism Inhibiting BCG and Mycobacterium Tuberculosis Survival in Infected Macrophages." *Cell*, U.S. National Library of Medicine, 17 Dec. 2004, www.ncbi.nlm.nih.gov/pubmed/15607973/.
33. Griffin, Laura M et al. "Human papillomavirus infection is inhibited by host autophagy in primary human keratinocytes." *Virology* vol. 437,1 (2013): 12-9. doi:10.1016/j.virol.2012.12.004
34. Sir, Donna, et al. "Induction of incomplete autophagic response by hepatitis C virus via the unfolded protein response." *Hepatology (Baltimore, Md.)* vol. 48,4 (2008): 1054-61. doi:10.1002/hep.22464
35. Shrivastava, Shubham, et al. "Knockdown of autophagy enhances the innate immune response in hepatitis C virus-infected hepatocytes." *Hepatology (Baltimore, Md.)* vol. 53,2 (2011): 406-14. doi:10.1002/hep.24073